

# Reduction of molecular ion interferences with hexapole collision cell in direct injection nebulization–inductively coupled plasma mass spectrometry

S. E. O'Brien,<sup>a,b</sup> B. W. Acon,<sup>a,b</sup> S. F. Boulyga,<sup>b†</sup> J. S. Becker,<sup>b</sup> H.-J. Dietze<sup>b</sup> and Akbar Montaser<sup>\*a</sup>

www.rsc.org/jaas

<sup>a</sup>Department of Chemistry, George Washington University, Washington, DC 20052, USA.  
E-mail: montaser@gwu.edu; Fax: 202-994-2298; Tel: 202-994-6480

<sup>b</sup>Central Department of Analytical Chemistry, Research Centre Juelich, D-52425 Juelich, Germany

Received 16th September 2002, Accepted 23rd January 2003

First published as an Advance Article on the web 5th February 2003

A hexapole collision cell was investigated for significant reductions of interferences by molecular ions in inductively coupled plasma mass spectrometry (ICPMS) using a direct injection high efficiency nebulizer (DIHEN). Collision induced reactions with hydrogen reduced isobaric interferences while the addition of helium as a collision gas enhanced analyte ion transmission through collisional focusing. Improved figures of merit were obtained for elements (Ca, Fe, Cr, As, Se) that are typically difficult to analyze with conventional quadrupole instruments. Sensitivities achieved with the DIHEN were higher (by factors ranging from 2 to 9) than those observed with a micronebulizer-spray chamber arrangement. Precision and detection limits were similar to or slightly improved over values obtained using the micronebulizer-spray chamber arrangement. The technique was successfully applied to the determination of Fe, Cr, Co, Cu, Pb, Al, Mn, Zn, Ag, and Sr on silicon wafer surfaces at a concentration range of  $(0.49\text{--}6.5) \times 10^9$  atoms  $\text{cm}^{-2}$ , sampled by a 100  $\mu\text{L}$  drop of  $\text{H}_2\text{O}\text{--}\text{H}_2\text{O}_2\text{--}\text{HF}$ , as well as for the determination of Cr in DNA.

## Introduction

Argon inductively coupled plasma mass spectrometry (Ar ICPMS) offers low detection limits ( $\text{ng L}^{-1}$  range and lower), a wide linear dynamic range (6–8 orders of magnitude), and good precision ( $<5\%$ ) for over 70 elements.<sup>1,2</sup> One of the main drawbacks of Ar ICPMS in practical applications is the presence of isobaric mass interferences between atomic ions.<sup>3,4</sup> Such interferences can be corrected in some cases, but with a sacrifice of both accuracy and precision. Alternatively, less abundant interference-free isotopes of the elements can be used for measurements, but sensitivity and detection limits will suffer. For determinations at trace levels, polyatomic interferences from plasma species (argides) and solvent species (oxides) are exceptionally problematic. For instance, the three isotopes of iron, <sup>54</sup>Fe, <sup>56</sup>Fe, and <sup>57</sup>Fe, as well as the <sup>75</sup>As mono-isotope, suffer from interferences from argon species (<sup>40</sup>Ar<sup>14</sup>N<sup>+</sup>, <sup>40</sup>Ar<sup>16</sup>O<sup>+</sup>, <sup>40</sup>Ar<sup>16</sup>OH<sup>+</sup>, and <sup>40</sup>Ar<sup>35</sup>Cl<sup>+</sup>, respectively). Relatedly, ionic species <sup>40</sup>Ar<sup>+</sup>, <sup>40</sup>ArH<sup>+</sup>, <sup>40</sup>Ar<sup>12</sup>C<sup>+</sup>, and <sup>40</sup>Ar<sup>40</sup>Ar<sup>+</sup>, reside at the same nominal masses as the isotopes <sup>40</sup>Ca<sup>+</sup>, <sup>41</sup>K<sup>+</sup>, <sup>52</sup>Cr<sup>+</sup>, and <sup>80</sup>Se<sup>+</sup>, respectively, thereby making trace element determination of these isotopes in complex matrices extremely difficult.

Several approaches have been explored to reduce, eliminate, or resolve isobaric interferences including sector field ICPMS,<sup>5–7</sup> applications of cold plasma<sup>8–10</sup> and a graphite injector tip,<sup>11</sup> solvent and matrix removal,<sup>12,13</sup> alternative plasma sources,<sup>14–18</sup> changes in interface design<sup>19</sup> and ion optics,<sup>20,21</sup> and collision and reaction cells.<sup>22–35</sup> These approaches have their own benefits and limitations. For example, sector field ICPMS offers resolving power ( $m/\Delta m$ ) up to 12,000 to separate most interferences of molecular ions from analyte ions, but at the expense of reduced

sensitivity and greater complexity of operation and maintenance. The main drawbacks of the cold plasma approach include reduced plasma robustness, increased matrix effects and poor figures of merit for most elements, especially those possessing high ionization potential ( $>8$  eV).<sup>6–10</sup> Sample preparation techniques are very effective in some cases for solvent or matrix removal, but they are usually time consuming and increase the risk of analyte loss and contamination. Alternative plasma sources such as helium plasmas provide enhanced levels of aerosol desolvation–vaporization, improved degrees of ionization for hard-to-ionize elements, and reduced mass spectral interferences. However, helium plasmas currently exhibit relatively low electron number density and low gas temperature compared to ICP discharges in Ar.<sup>15,16</sup>

The principles behind the collision cell concept and their applications were outlined for high-energy, multiply charged beams<sup>36</sup> before ICPMS became a widely used analytical technique. Initial experiments to attenuate interferences of molecular and analyte ions in Ar ICPMS were achieved by using a triple quadrupole MS,<sup>22</sup> and an rf-only quadrupole as the first stage of a double quadrupole arrangement.<sup>23</sup> In general, collisional focusing would be realized if the neutral gas introduced to the rf-multipole collision cell possesses a lower molecular weight than the analyte ions.<sup>37</sup> Ion focusing, due to the kinetic energy distribution relaxation of the ions, results in enhanced ion transmission.<sup>25–27</sup> Alternatively, inducing specific reactions between the interfering ion and the collision cell gas can simply remove the interfering ion to a different  $m/z$ .<sup>29–35</sup> In general, collision or reaction cell-based ICPMS instruments create cell conditions, under normal plasma conditions, for measuring the most abundant isotopes of the elements, including difficult elements [K ( $m/z = 39$ ), Ca ( $m/z = 40$ ), and Fe ( $m/z = 56$ )] that are typically measured in cool plasmas.<sup>35,38</sup> An excellent review examines the recent literature relating to the history, design, operation and application of

<sup>†</sup>On leave from The Radiation Physics and Chemistry Problems Institute, 220109, Sosny, Minsk, Belarus.

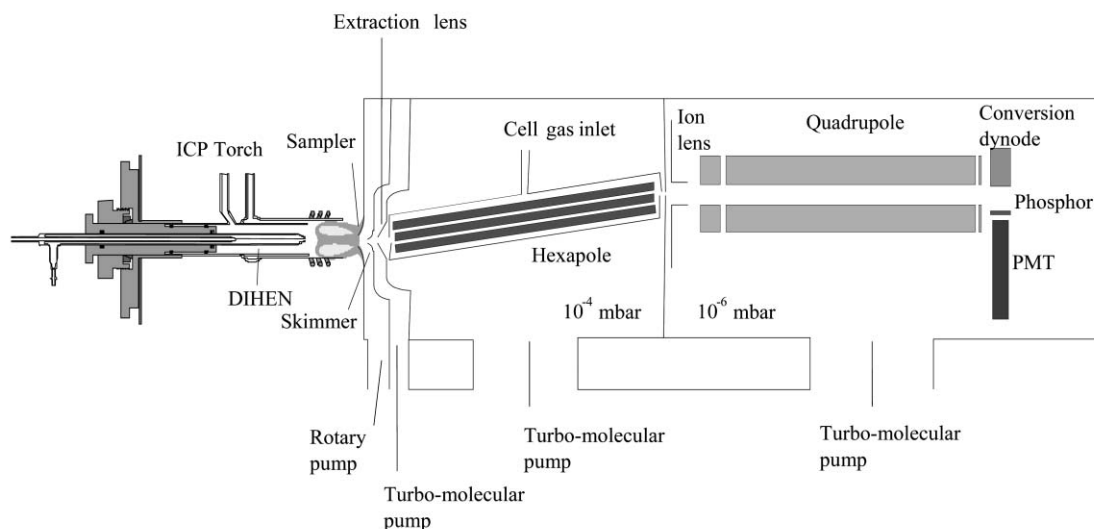


**Fig. 1** Schematic diagram of Platform ICPMS with hexapole collision cell and shielded torch using a DIHEN for solution introduction.

multipole collision cells and reaction cells in combination with ICPMS along with the fundamentals of ion collision and reaction, including thermochemistry, energy transfer and reaction kinetics.<sup>39</sup>

The objective of this study was to explore the capability of ICPMS with collision cell for the direct injection of a microliter volume of test sample to the plasma, with and without the shielded torch, and to find conditions for the simultaneous detection of a wide range of elements that are traditionally measured under hot and cool plasma conditions. A direct injection high efficiency nebulizer (DIHEN) was used as the sample introduction device,<sup>40–49</sup> rather than the conventional nebulizer-spray chamber arrangement. The study with the DIHEN is important because the collision cell technology has the potential to provide sufficiently low detection limits for certain key applications, where the sample is often expensive (*e.g.*, semiconductor chemicals), highly hazardous (*e.g.*, radioactive materials), or limited in volume (*e.g.*, biological samples, chromatographic applications). The DIHEN offers several advantages over conventional solution introduction devices, including low sample consumption ( $1\text{--}100\ \mu\text{L min}^{-1}$ ) and nebulizer gas flow ( $0.2\ \text{L min}^{-1}$ ), 100% analyte transport efficiency, reduced memory effects, and no loss of volatile analytes.<sup>40</sup> The aim of this work was to explore the effects of hydrogen (as the reactant gas) and helium (as the buffer gas)

for reducing major mass interferences by molecular ions. The influence of the negative dc bias potential applied to the hexapole was also examined for reducing interferences produced within the collision cell. Finally, the applicability of the DIHEN with collision cell ICPMS was tested by measuring metal surface contamination (Fe, Cr, Co, Cu, Pb, Al, Mn, Zn, Ag, and Sr) on silicon wafer samples and Cr bound to DNA. As far as we know, this report constitutes the first account of characterizing a collision cell ICPMS for direct injection solution introduction.

## Experimental

### Instrumentation

A Platform ICPMS instrument, with a hexapole collision cell, was used (Micromass Ltd., Manchester, UK). The collision cell was operated with helium as the buffer gas and hydrogen as the reactant gas. A schematic diagram of the instrument is given in Fig. 1, along with operating conditions in Table 1. A shielded torch was coupled to the instrument between the load coil and the torch to reduce rf coupling to the plasma and improve sensitivity (Table 2). The instrument is also equipped with a Daly-type photomultiplier detector, operating in the analogue mode. To express sensitivity (MHz per ppm), the analog output is converted to counts by the instrument using an algorithm.<sup>50</sup>

**Table 1** Operating conditions for the collision cell ICPMS instrument

<i>Sample introduction systems</i>	DIHEN (Model 170-AA), Micromist-minicyclonic cinnabar spray chamber
Solution uptake rate/ $\mu\text{L min}^{-1}$	60 (DIHEN), 285 (Micromist-minicyclonic cinnabar spray chamber)
Injector gas flow rate/ $\text{L min}^{-1}$	0.18 (DIHEN), 0.70 (Micromist-minicyclonic cinnabar spray chamber)
DIHEN position below the torch intermediate tube/mm	2
<i>ICPMS system</i>	Micromass Platform ICPMS with hexapole collision cell
Rf generator type	Crystal controlled, 27 MHz
Induction coil circuitry	3-turn coil
Shielded torch	Fixed, platinum
Rf power/W	1350
Rf generator frequency	27
Outer gas flow rate/ $\text{L min}^{-1}$	13.5
Intermediate gas flow rate/ $\text{L min}^{-1}$	1.2
Sampling depth (above load coil)/mm	11
Sampler (orifice diameter/mm)	Nickel (1.1)
Skimmer (orifice diameter/mm)	Nickel (0.9)
Helium collision cell gas flow/ $\text{mL min}^{-1}$	1–10
Hydrogen collision cell gas flow/ $\text{mL min}^{-1}$	1–10
Hexapole dc bias potential/V	–10–0
Cone (extraction lens)/V	–400–600
Hexapole exit lens/V	–400
Ion energy lens/V	–2

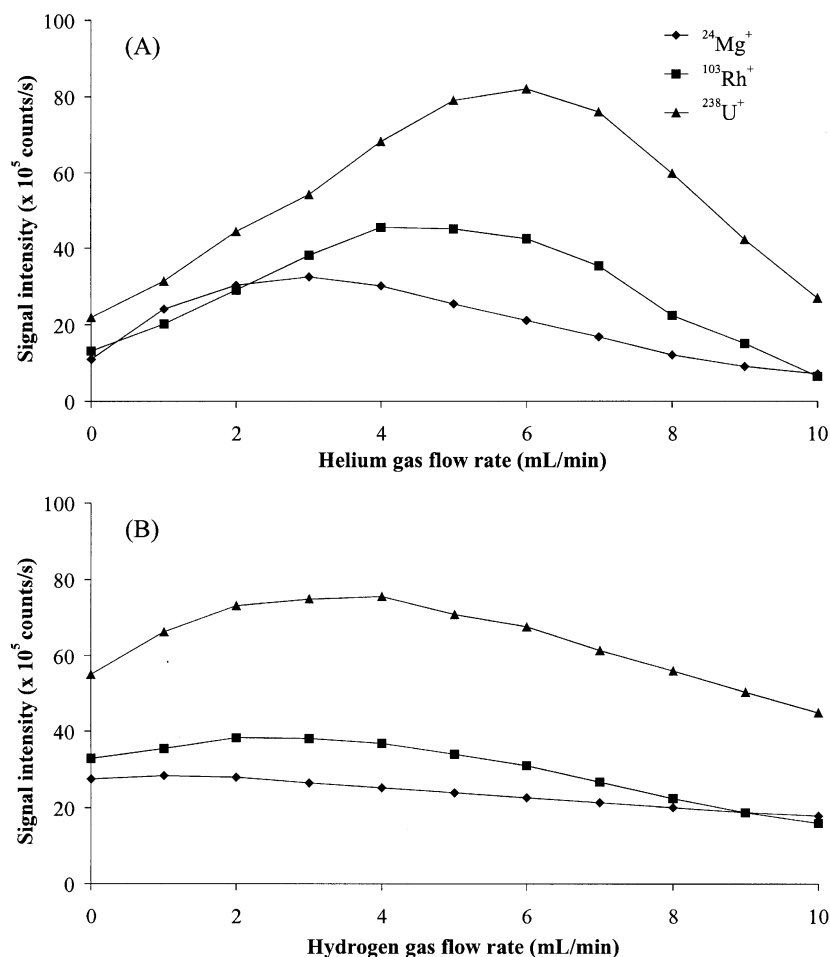


**Fig. 2** Influence of (A) helium and (B) hydrogen collision cell gas flow rates on analyte ion intensity for introduction of a  $10 \text{ ng mL}^{-1}$  solution of Mg, Rh, U with the DIHEN. Hexapole bias potential was set at 0 V (Fig. 2(A): Hydrogen =  $0 \text{ mL min}^{-1}$ , Fig. 2(B): helium =  $5 \text{ mL min}^{-1}$ ).

### Nebulization systems

Two nebulizers are used, a DIHEN<sup>51</sup> (Model 170-AA, J E Meinhard<sup>®</sup> Associates Inc., Santa Ana, CA) and a Micromist nebulizer equipped with a 20-mL minicyclonic cinnabar spray chamber (Model MicroMist AR40-1-FM01, Glass Expansion Ltd., Hawthorn, Victoria, Australia). Sample delivery is achieved *via* a four-channel peristaltic pump (Minipuls 3, Gilson, Villiers le Bel, France). The instrument controlled the nebulizer gas flow internally.

The DIHEN replaces the injector tube of a demountable ICP torch. A PEEK adapter was constructed to hold the DIHEN in the center of the demountable ICP torch 2 mm below the intermediate torch tube. The dead volume of the nebulizer was reduced to  $<10 \mu\text{L}$  by inserting 0.008"-id tubing (SB Fittings Assembly Kit #1-Micro, J E Meinhard Associates, Inc.) into the nebulizer to the point where the solution capillary tapers. Because the torch is isolated within a relatively large instrument cabinet, about 2 feet of tubing is necessary to deliver the solution to the nebulizer. This arrangement results in increased solution waste.

### Reagents and sample preparation

Standard solutions were prepared from  $1000 \mu\text{g mL}^{-1}$  stock solutions of the element (Merck, Darmstadt, Germany) and  $18 \text{ M}\Omega \text{ cm}$  deionized water. Silicon wafer samples were obtained from the Research Centre Juelich and analyzed for metal surface contamination. The vapor phase decomposition (VPD) technique was used to etch the silicon oxide layer by exposure to HF vapor.<sup>52</sup> A  $100\text{-}\mu\text{L}$  drop of  $\text{H}_2\text{O-H}_2\text{O}_2\text{-HF}$  was then used to scan the surface and dissolve surface contaminants.

This drop was then diluted to 2 mL and analyzed using the standard addition technique. It is important to note that the DIHEN should not be operated with high HF concentrations. In this case, the solution contained 0.05% HF, resulting in no damage to the nebulizer. The Cr bound to DNA samples were prepared as described elsewhere<sup>40,42</sup> and analyzed using a 3-point standard addition technique. These samples were obtained from Professor Steven R. Patierno (Department of Pharmacology, The George Washington University).

### DIHEN operating conditions with collision cell hexapole ICPMS instrument

Optimum solution uptake rate, RF power, and nebulizer gas flow rate were determined based on the maximum ion intensity of the analytes for nebulization of  $10 \text{ ng mL}^{-1}$  multi-element solution with the DIHEN. The optimum operating conditions generally show a mass dependence. The following conditions were used to measure figures of merit and for the analysis of silicon wafers and Cr-bound DNA with the DIHEN: a nebulizer gas flow rate of  $0.18 \text{ L min}^{-1}$ , an RF power of 1350 W and a solution uptake rate of  $60 \mu\text{L min}^{-1}$ .

## Results and discussion

### Influence of collision cell gases on analyte ion signal

Fig. 2 shows the effects of the collision cell gases on analyte signal intensities. The maximum ion intensity of analytes was achieved at a helium flow of  $5 \text{ mL min}^{-1}$  (no hydrogen was introduced into the cell, Fig. 2(A)). Under this condition, the

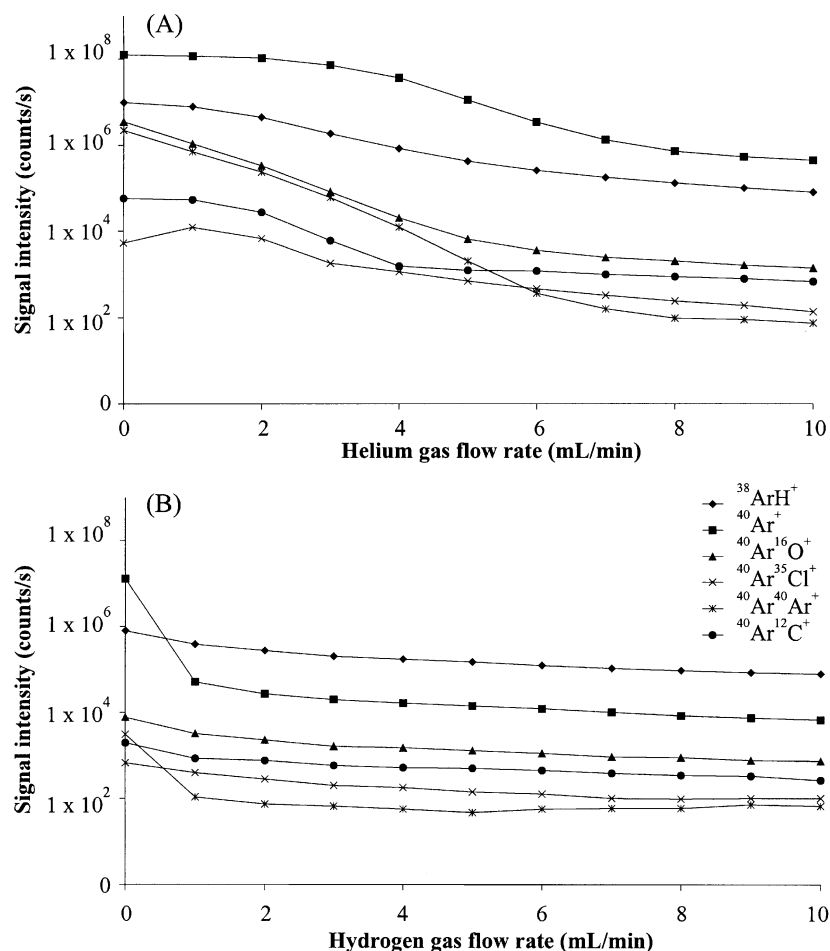


**Fig. 3** Influence of (A) helium and (B) hydrogen collision cell gas flow rates on argon molecular ion intensity for the introduction of deionized water with the DIHEN. Hexapole bias potential was set at -2 V (Fig. 2(A): hydrogen = 0 mL min<sup>-1</sup>; Fig. 2(B): helium = 5 mL min<sup>-1</sup>).

hydrogen gas flow was varied to achieve best analyte ion intensity (Fig. 2(B)). The analyte ion intensities are enhanced by a factor of 3–4 with the addition of helium to the cell. The increase in intensity is attributed to collision of the ions with the neutral molecules of the collision cell gas causing the ions to lose kinetic energy, change their trajectory, and be focused to the central axis of the rf hexapole. The optimum collision cell gas flow rate depends not only on the mass of the analyte ion but also on the nature of the gases present in the collision cell. The relative mass of the ion and neutral buffer species plays a crucial role in achieving efficient ion thermalization,<sup>26</sup> as is illustrated by the mass dependence observed with respect to optimum collision cell gas flow rate (Fig. 2). Collisions would lead to negligible loss of analyte ions for a collision cell gas having low molecular weight while ion scattering would result if the molecular weight of the collision cell gas is too high, *i.e.*, comparable with the mass of the analyte ion. The optimum flow rates for Mg, Rh, and U were 3, 4, and 6 mL min<sup>-1</sup>, respectively. At higher pressures (higher collision cell gas flow rates), lower mass ions were more susceptible to ion scattering, and thus reduced ion transmission and intensities. For hydrogen, the optimum gas flow rates are 1, 3, and 4, respectively, for Mg, Rh, and U, corresponding to lower intensity enhancement due to a higher total gas flow rate of 6, 8, and 9 in the collision cell. Similar trends and enhancement factors (up to a factor of 4) are observed for this instrument using a Micromist nebulizer with minicyclonic spray chamber. These results are also in agreement with published work involving a Meinhard nebulizer cooled spray chamber arrangement,<sup>53</sup> except that analyte ion intensities were improved by a factor of 10.

#### Influence of collision cell gases on argon molecular ion intensity

Fig. 3 shows the dependence of the intensities of several molecular and atomic ions of argon (<sup>38</sup>ArH<sup>+</sup>, <sup>40</sup>Ar<sup>+</sup>, <sup>40</sup>Ar<sup>12</sup>C<sup>+</sup>, <sup>40</sup>Ar<sup>16</sup>O<sup>+</sup>, <sup>40</sup>Ar<sup>35</sup>Cl<sup>+</sup>, and <sup>40</sup>Ar<sup>40</sup>Ar<sup>+</sup>) on the collision cell gas flow rates for the introduction of deionized water. These six ionic species caused by the plasma gas typically hinder the determination of <sup>39</sup>K, <sup>40</sup>Ca, <sup>52</sup>Cr, <sup>56</sup>Fe, <sup>75</sup>As, and <sup>80</sup>Se, respectively. The addition of helium or hydrogen to the collision cell generally results in a reduction of the argon molecular ion intensity by 1–4 orders of magnitude due to the loss of energy in the cell such that transport into the mass analyzer is discriminated. In other words, argon molecular ions exit the collision cell, but do not enter the mass analyzer because of energy discrimination. In general, a decrease in ion intensity is observed with the addition of helium to the cell for the following reasons. First, the energy of the ions derived from the argon ICP is decreased to a value below 1 eV by collision with helium atoms.<sup>54</sup> Molecular ions are moderated even more efficiently than single-atom ions due to slightly higher scattering cross sections. Second, even if no reactive gas (*e.g.*, hydrogen) is introduced into the collision cell, the hydrogen originating from the water dissociated in the ICP is entrained into the collision cell,<sup>55</sup> an entrainment that increases for direct injection solution introduction. Third, at lower kinetic energies, the reaction rate of argon ions and argon molecular ions with hydrogen residues increases, leading to the reduction of their intensities. An additional reduction is caused by collisional fragmentation of molecular ions<sup>56</sup> and by greater energy discrimination at higher helium flow rate (see Fig. 2).

With the addition of hydrogen, the argon molecular ions react with hydrogen through charge transfer, proton transfer,

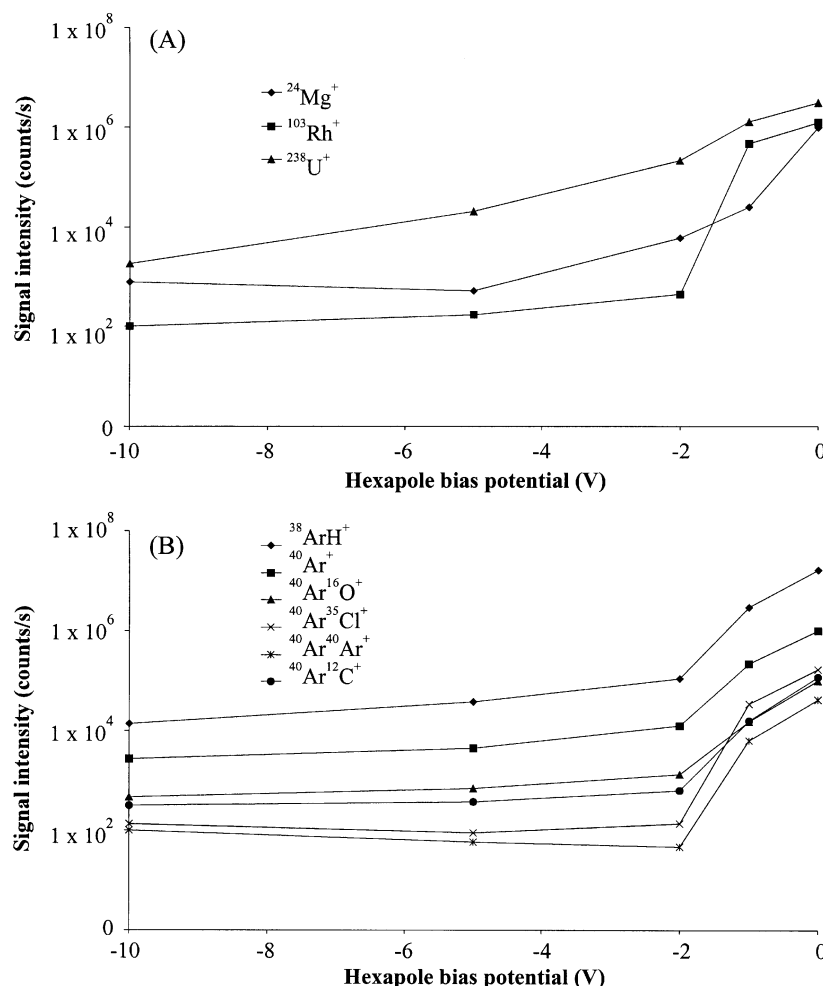


**Fig. 4** Influence of hexapole bias potential on (A) analyte ion and (B) argon molecular ion intensities for introduction of a  $10 \text{ ng mL}^{-1}$  solution of Mg, Rh, U, and deionized water, respectively, using the DIHEN (helium =  $5 \text{ mL min}^{-1}$ , hydrogen =  $5 \text{ mL min}^{-1}$ ).

or hydrogen atom transfer, resulting in the production of new ions or neutral species at  $m/z$  other than the  $m/z$  of the analyte ion.<sup>29–32</sup> Reduction in kinetic energy due to collision with gas atoms also serves to increase the cross section of the gas phase reactions,<sup>56</sup> and thus facilitates the use of thermal ion–molecule chemistry.<sup>55</sup> The argon molecular ion intensities were reduced by up to 4 orders of magnitude for the DIHEN (Fig. 3), compared with 3 orders of magnitude for the Micromist nebulizer-cyclonic spray chamber and previous studies involving conventional sample introduction systems.<sup>31,32,53</sup>

#### The effect of hexapole bias potential on the analyte and argon molecular ion intensities

In addition to collision cell gases, the application of a negative hexapole bias potential, relative to the quadrupole, also plays a significant role in reducing the intensities of the argon molecular ions (Fig. 4). These measurements were conducted with  $5 \text{ mL min}^{-1}$  helium and  $5 \text{ mL min}^{-1}$  hydrogen present in the collision cell and with the introduction of deionized water with the DIHEN. For both the analyte ion and the argon molecular ion intensities, a sharp decrease is observed at negative dc hexapole bias potentials by 2–4 orders of magnitude, with the maximum intensities appearing at 0 V. At a dc bias potential of 0 to  $-2 \text{ V}$ , the signal-to-background and the signal-to-noise ratios of the analyte ions (data not shown) are improved, especially for difficult-to-analyze elements. The observed decrease of ion intensity (Fig. 4) was caused by the negative dc hexapole bias potential relative to the quadrupole, which creates an energy barrier for ions exiting the hexapole. Consequently, ions with reduced

kinetic energy are suppressed due to collision with cell gases. A possible reason for the improvement of signal-to noise ratio might be the more efficient moderation of molecular ions in comparison with single-atom ions (analyte ions in this case). In addition, the intensity of molecular ionic species, mainly water, hydrocarbons<sup>31</sup> or complex cluster ions originating from matrix and water residues, formed by collision-induced reactions in the cell, are decreased by the application of a negative dc hexapole bias potential barrier, which reduces transmission into the mass filter.<sup>31,57,58</sup> These residual gas ions possess lower kinetic energies than the analyte ions since they are produced within the cell, as opposed to the analyte ions, which are formed in the ICP. Thus, analyte ions are transmitted much more effectively than the residual ions. Similar responses to the application of a negative dc hexapole bias potential have been previously reported for a conventional nebulization system.<sup>53</sup> A mass dependence of analyte ion intensity on hexapole bias potential has also been reported<sup>53</sup> due to the difference in kinetic energy of different mass ions; however, no significant mass dependence was observed here.

#### Influence of collision cell gases and hexapole bias potential on $\text{MO}^+/\text{M}^+$

The effects of the collision cell gases and hexapole bias potential on the  $\text{MO}^+/\text{M}^+$  ratio are presented in Fig. 5 for Ce. At  $-2 \text{ V}$ , the  $\text{CeO}^+/\text{Ce}^+$  ratio decreases for the DIHEN with increasing helium flow in the collision cell, similar to conventional nebulization.<sup>24,53</sup> This is due to a greater loss of kinetic energy by the  $\text{CeO}^+$  oxide ion, leading to more effective energy discrimination at the mass filter, compared to the  $\text{Ce}^+$

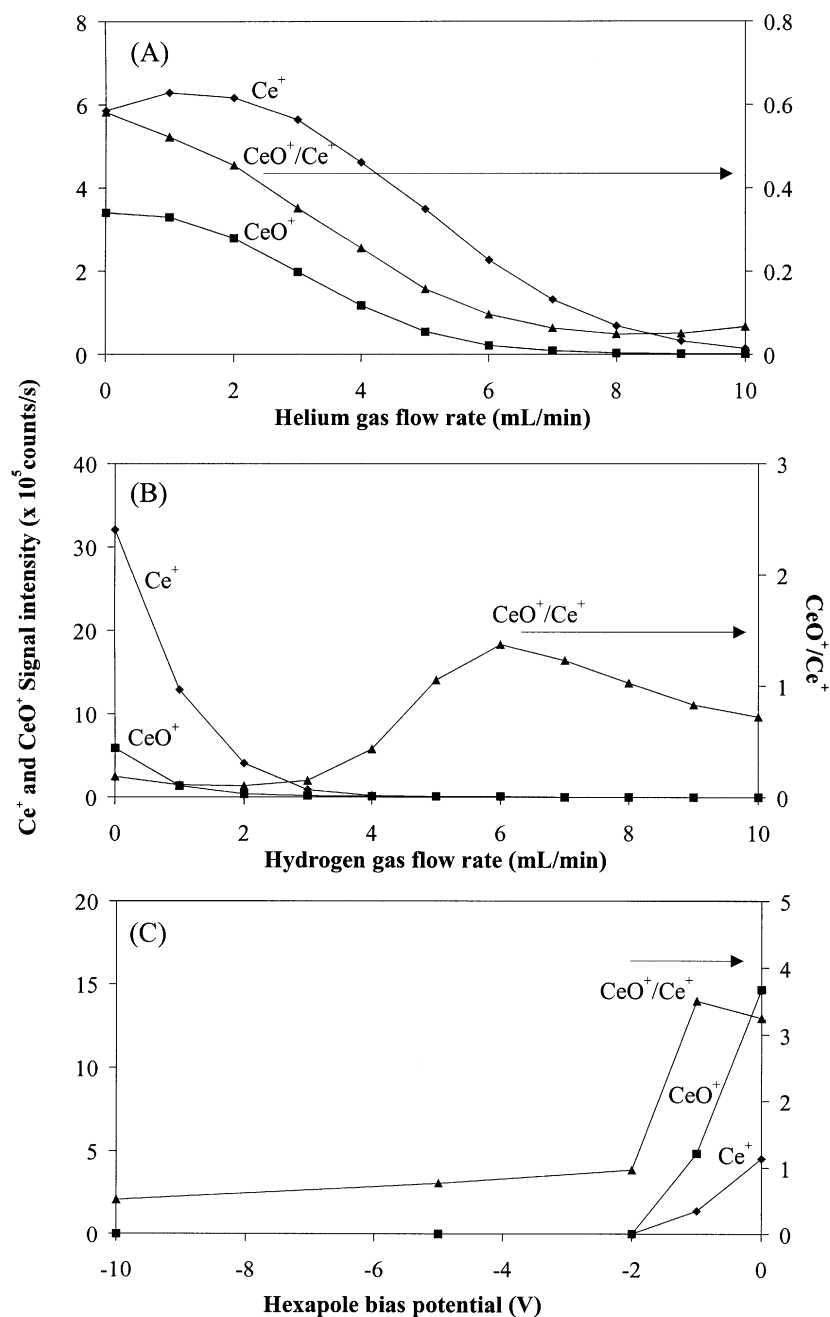


**Fig. 5** Influence of (A) helium and (B) hydrogen collision cell gas flow rates and (C) hexapole bias potential on  $\text{CeO}^+/\text{Ce}^+$  ratios with the DIHEN. For A and B, hexapole bias potential =  $-2$  V. For C, helium =  $5 \text{ mL min}^{-1}$  and hydrogen =  $5 \text{ mL min}^{-1}$ .

analyte ion. With the introduction of hydrogen to the collision cell, both the  $\text{Ce}^+$  and  $\text{CeO}^+$  intensities decrease sharply: however, the  $\text{CeO}^+/\text{Ce}^+$  ratio decreases only slightly initially and then increases significantly at  $4 \text{ mL min}^{-1}$  of hydrogen. This initial decrease in oxide ratio may also be attributed to enhanced kinetic energy loss (and energy discrimination at the quadrupole) of the  $\text{CeO}^+$  ion, as well as its reaction with hydrogen.<sup>24</sup> Published work with conventional sample introduction systems reports a reduction in oxide ratios with the addition of hydrogen to the collision cell.<sup>24,53</sup> The reason for this disparity requires further investigation. The application of a negative hexapole bias potential reduces  $\text{CeO}^+/\text{Ce}^+$  ratios, similar to that observed with conventional nebulizers.<sup>24,53</sup> Thus, in order to minimize oxide ratios, the DIHEN should be operated with the collision cell having high helium gas flow rates ( $> 5 \text{ mL min}^{-1}$ ), low hydrogen gas flow rates ( $< 5 \text{ mL min}^{-1}$ ) and a negative dc hexapole bias potential (0 to  $-2$  V), conditions which also favor the determination of difficult-to-analyze elements, but with a substantial sacrifice of ion intensities.

With direct injection nebulization, high oxide ratios are typically observed, for instance 48% for  $\text{CeO}^+/\text{Ce}^+$ ,<sup>40</sup> due to the increased solvent load in the ICP. However, under optimum collision cell conditions of  $6 \text{ mL min}^{-1}$  helium,  $4 \text{ mL min}^{-1}$  hydrogen, and  $-2$  V hexapole bias potential, oxide ratios are reduced to 20%. Oxide ions of lower bond strength,<sup>24</sup> for instance 3.8 eV for  $\text{YbO}^+$  (compared to 8.8 eV for  $\text{CeO}^+$ ), show greater improvements in  $\text{MO}^+/\text{M}^+$ , from 3% to 0.4%.

#### Figures of merit

Sensitivity, detection limits, and precision are presented in Table 2 for 21 isotopes across the mass range, using the DIHEN and a Micromist nebulizer–minicyclonic cinnabar spray chamber arrangement. Considering that this instrument operates in the analogue mode, the signal output is converted to counts by the instrument to express sensitivity ( $\text{MHz ppm}^{-1}$ ).<sup>50</sup> Sensitivities obtained with the DIHEN are 2–9 times greater than those obtained with the Micromist nebulization

**Table 2** Sensitivity (MHz ppm<sup>-1</sup>), detection limit (ng L<sup>-1</sup>), and precision (% RSD) for two nebulization systems, obtained with and without shielded torch (ST). Helium flow rate = 6 mL min<sup>-1</sup>, hydrogen flow rate = 4 mL min<sup>-1</sup>, hexapole bias potential = 0 V

	DIHEN						Micromist-minicyclonic spray chamber					
	Sensitivity		Detection limit <sup>b</sup>		Precision <sup>a</sup>		Sensitivity		Detection limit <sup>b</sup>		Precision <sup>a</sup>	
	ST	No ST	ST	No ST	ST	No ST	ST	No ST	ST	No ST	ST	No ST
<sup>9</sup> Be	30	21	7	5	2	0.3	10	4	11	31	11	2
<sup>24</sup> Mg	280	103	9	10	0.5	2	121	45	6	14	0.7	2
<sup>40</sup> Ca	1225	346	7	22	2	0.5	253	95	6	36	3	2
<sup>52</sup> Cr	583	181	0.8	2	2	0.4	265	100	1	2	0.9	2
<sup>55</sup> Mn	908	234	0.7	1	1	0.6	409	129	0.5	1	0.9	1
<sup>56</sup> Fe	790	199	2	3	0.4	0.3	358	111	2	3	0.8	0.8
<sup>58</sup> Ni	979	37	9	60	0.3	0.3	105	57	18	8	2	1
<sup>59</sup> Co	706	172	7	6	0.6	0.1	292	123	3	2	0.6	1
<sup>75</sup> As	210	37	10	10	1	0.3	50	18	10	4	1	0.7
<sup>80</sup> Se	72	21	4	6	3	0.5	106	35	2	3	4	4
<sup>88</sup> Sr	1697	285	0.4	1	2	0.7	561	155	0.6	1	1	1
<sup>89</sup> Y	647	195	0.3	0.7	2	0.6	165	116	1	1	7	1
<sup>103</sup> Rh	2203	361	0.2	0.5	3	0.8	796	181	0.3	0.6	1	2
<sup>114</sup> Cd	658	90	0.4	2	3	1	231	39	2	6	0.9	0.8
<sup>138</sup> Ba	3034	591	0.2	0.5	2	1	647	159	0.6	2	2	0.9
<sup>139</sup> La	2729	848	0.1	0.2	3	1	497	231	0.4	0.8	12	2
<sup>140</sup> Ce	3267	753	0.1	0.3	2	0.5	684	233	0.4	0.9	8	2
<sup>184</sup> W	698	81	0.7	2	2	0.7	261	32	0.4	1	2	1
<sup>208</sup> Pb	1664	147	0.1	0.6	2	0.5	538	65	2	3	1	1
<sup>238</sup> U	740	216	0.1	0.1	3	0.9	521	89	0.4	1	8	0.7
Average RSD					1.8	0.6					3.2	1.4

<sup>a</sup>N = 5 for concentration of 10 ng mL<sup>-1</sup> multi-element solution. <sup>b</sup>Based on 3σ of the blank solution measured at the mass of the analyte.

**Table 3** Analysis of SRM 1643d (Trace elements in water) and silicon wafer samples using DIHEN-collision cell ICPMS<sup>a</sup>. Helium flow rate = 8 mL min<sup>-1</sup>, hydrogen flow rate = 1.5 mL min<sup>-1</sup>, hexapole bias potential = -2 V

Analyte isotope	Trace elements in water		Silicon wafer samples	
			1	2
	<i>Certified</i> ng mL <sup>-1</sup>	<i>Found</i> ng mL <sup>-1</sup>	<i>Atoms</i> × 10 <sup>9</sup> /cm <sup>2</sup>	<i>Atoms</i> × 10 <sup>9</sup> /cm <sup>2</sup>
<sup>56</sup> Fe	91.2 ± 3.9	93.4 ± 4.8	1.4	2.9
<sup>52</sup> Cr	18.53 ± 0.2	18.98 ± 0.6	3.8	0.74
<sup>59</sup> Co	25 ± 0.59	—	2.1	4.0
<sup>64</sup> Cu	20.5 ± 3.8	19.9 ± 1.6	2.2	2.7
<sup>208</sup> Pb	18.15 ± 0.64	17.78 ± 0.9	—	5.4
<sup>27</sup> Al	127.6 ± 3.5	130.7 ± 4.2	5.0	6.5
<sup>55</sup> Mn	37.66 ± 0.83	37.9 ± 0.2	3.3	0.49
<sup>65</sup> Zn	72.48 ± 0.65	71.35 ± 1.1	—	3.1
<sup>108</sup> Ag	1.27 ± 0.057	1.24 ± 0.02	1.9	1.1
<sup>88</sup> Sr	294.8 ± 3.4	292 ± 4.1	1.6	2.0

<sup>a</sup>Operating conditions are given in Table 1.

system, both with and without the shielded torch. The use of the shielded torch improves sensitivity by up to an order of magnitude with the DIHEN, and up to a factor of 8 with the Micromist. With the DIHEN, the precision values obtained are generally better in the absence of the shielded torch, rather than with the shielded torch. Further, the DIHEN provides precision values that are similar to or better than (typically 2–3 times) those obtained with the Micromist nebulizer. Importantly, the precision data obtained for the DIHEN in this work using the shielded torch are not as favorable as our previous data obtained with an ICPMS instrument equipped with an electronically balanced RF generator circuit,<sup>40,44,45</sup> suggesting that the latter technology currently offers a more dynamic system for handling the generally large solvent load introduced through direct injection. If no shielded torch is utilized, the DIHEN provides precision values that are similar to those obtained with an ICPMS system having an electronically balanced rf generator circuit,<sup>40,44,45</sup> but the sensitivity is reduced by up to an order of magnitude in the absence of the shielded torch. Further work is essential on the reduction of the solvent load from the DIHEN or increasing the speed of the

matching network involving the shielded torch to improve precision without sacrificing sensitivity improvement.

Despite the large increase in sensitivity achieved with the shielded torch, the detection limits obtained are similar to or only slightly better than those obtained when no shielded torch is utilized due to the lower precision obtained with the shielded torch. The detection limits measured using the DIHEN were generally similar to those obtained with the Micromist nebulizer. In both cases, detection limits for difficult to analyze elements were improved by as much as 3 orders of magnitude over those obtained with non-cell quadrupole ICPMS instruments.<sup>53</sup>

In this work, the DIHEN-collision cell ICPMS was used for metal ion recovery studies using SRM 1643d (Trace elements in water). The results of this, given in Table 3, indicate good agreement between the certified and recovered values, with the largest deviation showing 3% error.

#### Determination of metal impurities on silicon wafer surfaces

Contamination is a major problem in the semiconductor industry during integrated circuit (IC) production. In particular,

metal contamination at even ultra-trace levels can alter the electric properties of the ICs. The maximum level of contamination must be reduced to produce smaller ICs, thus analytical techniques with very low detection capabilities (sub pg L<sup>-1</sup>) are required. Silicon wafer samples, obtained from the Research Center Juelich, were also analyzed for metal ion surface contamination. Since metal concentrations are already quite low, it is necessary to avoid large sample dilutions. Thus, such applications require the analysis of very small sample volumes, preferably with direct injection micro-nebulizers such as the DIHEN. In this work, the total volume of sample available for analysis, before dilution, was 100 µL. The sample was then diluted to 2 mL with deionized water and analyzed using a 3-point standard addition technique. Results of these studies (Table 3) show concentrations of the order of 0.5–6.5 × 10<sup>9</sup> atoms cm<sup>-2</sup> for two samples taken from the same wafer. Variations are possibly due to spatial disparity in the surface contamination.

### Determination of Cr in DNA

Another application well suited for the DIHEN-collision cell-ICP-MS technique is the analysis of expensive small volume biological samples, namely Cr bound to human DNA. Chromium(vi) from industrial effluents, like those from the electroplating, steel, and textile industries, is regulated by the US EPA as a known carcinogen, causing both lung and kidney cancer. Traditionally, DNA bound Cr is determined using radioactive <sup>51</sup>Cr bound with DNA and using a scintillation detector.<sup>59</sup> However, the Cr adduct levels are of the order of only several Cr atoms per 10,000 base pairs of DNA,<sup>60</sup> thus a very sensitive technique, like ICP-MS,<sup>42,43,46</sup> is required for biologically salient routine Cr-DNA assays. The analysis was conducted using a 3-point standard addition technique from a total volume of 2 mL of sample, prepared using a procedure similar to that described previously.<sup>40,42</sup> A concentration of 0.74 ± 0.1 ng mL<sup>-1</sup> Cr in DNA sample was obtained for 6 mL min<sup>-1</sup> helium, 4 mL min<sup>-1</sup> hydrogen and -2 V hexapole bias potential. A concentration of 0.75 ± 0.01 ng mL<sup>-1</sup> was obtained for the same sample using a double focusing sector field ICPMS operated at medium resolution ( $m/\Delta m$  of 3000).<sup>61</sup>

### Conclusions

A direct injection high efficiency nebulizer was coupled with a quadrupole ICPMS equipped with a hexapole collision cell to reduce or eliminate molecular ion interferences generally observed with argon plasmas, thus improving the figures of merit. This was achieved by the addition of hydrogen to the collision cell as a reactant gas, and helium as a buffer gas. As a result, signal to background ratios for several typically difficult-to-analyze elements were improved and MO<sup>+</sup>/M<sup>+</sup> ratios were significantly reduced. The use of the DIHEN-collision cell-ICPMS technique further improved the figures of merit for a number of analytes and allowed the successful analysis of silicon wafers for metal surface contamination in 100 µL of sample as well as chromium determination in DNA.

### Acknowledgements

Research at the George Washington University (GWU) was sponsored by grants from the US Department of Energy (DE-FG02-93ER14320), the National Science Foundation (CHE-9505726 and CHE-9512441), and J E Meinhard Associates, Inc. We acknowledge partial financial support for S. E. O'Brien and B. W. Acon through Central Department of Analytical Chemistry, Research Center Juelich, Germany. The authors are grateful to C. Pickhardt (Central Department of Analytical Chemistry, Research Centre Juelich) and John

A. McLean (GWU) for constructive discussions and assistance. We express our gratitude to Professor Steven R. Patierno, Dr. Jatinder Singh, and Mr. Daryl Pritchard (Department of Pharmacology, The George Washington University) for preparing and providing the Cr-DNA samples used in this research.

### References

- 1 A. Montaser, *Inductively Coupled Plasma Mass Spectrometry*, Wiley-VCH, New York, 1998.
- 2 A. Montaser and D. W. Golightly, *Inductively Coupled Plasma in Analytical Atomic Spectrometry*, Wiley-VCH, New York, 2nd edn., 1992.
- 3 S. H. Tan and G. Horlick, *Appl. Spectrosc.*, 1986, **40**, 445.
- 4 M. A. Vaughan and G. Horlick, *Appl. Spectrosc.*, 1987, **41**, 523.
- 5 B. Klaue and J. D. Blum, *Anal. Chem.*, 1999, **71**, 1408.
- 6 F. Vanhaecke, S. Saverwyns, G. D. Wannemacker, L. Moens and R. Dams, *Anal. Chim. Acta*, 2000, **419**, 55.
- 7 J. A. McLean, J. S. Becker, S. F. Boulyga, H.-J. Dietze and A. Montaser, *Int. J. Mass Spectrom.*, 2001, **208**, 193.
- 8 M. G. Minnich and A. Montaser, *Appl. Spectrosc.*, 2000, **54**, 1261.
- 9 S.-J. Jiang, R. S. Houk and M. A. Stevens, *Anal. Chem.*, 1988, **60**, 1217.
- 10 S. D. Tanner, M. Paul, S. A. Beres and E. R. Denoyer, *At. Spectrosc.*, 1995, **16**, 16.
- 11 P. S. Clemons, M. G. Minnich and R. S. Houk, *Anal. Chem.*, 1995, **67**, 1929.
- 12 A. Montaser, H. Tan, I. Ishii, S.-H. Nam and M. Cai, *Anal. Chem.*, 1991, **63**, 2660.
- 13 J. W. McLaren, J. W. Lam and A. Gustavsson, *Spectrochim. Acta, Part B*, 1990, **45**, 1091.
- 14 J. W. Lam and J. W. McLaren, *J. Anal. At. Spectrom.*, 1990, **5**, 419.
- 15 H. Zhang, S.-H. Nam, M. Cai and A. Montaser, *Appl. Spectrosc.*, 1996, **50**, 427.
- 16 S.-H. Nam, H. Zhang, M. Cai, J.-S. Lim and A. Montaser, *Fresenius' J. Anal. Chem.*, 1996, **355**, 510.
- 17 A. Montaser and H. Zhang, in *Inductively Coupled Plasma Mass Spectrometry*, ed. A. Montaser, Wiley-VCH, New York, 1998, ch. 10, pp. 809–890.
- 18 H. Zhang, A. Montaser, B. S. Zimmer, N. P. Vela and J. A. Caruso, in *Inductively Coupled Plasma Mass Spectrometry*, ed. A. Montaser, Wiley-VCH, New York, 1998, ch. 11, pp. 891–939.
- 19 D. J. Douglas and J. B. French, *J. Anal. At. Spectrom.*, 1988, **3**, 743.
- 20 K. Hu, P. S. Clemons and R. S. Houk, *J. Am. Soc. Mass Spectrom.*, 1993, **4**, 16.
- 21 K. Hu and R. S. Houk, *J. Am. Soc. Mass Spectrom.*, 1993, **4**, 28.
- 22 D. J. Douglas, *Can. J. Spectrosc.*, 1989, **34**, 38.
- 23 J. T. Rowan and R. S. Houk, *Appl. Spectrosc.*, 1989, **43**, 976.
- 24 Z. Du and R. S. Houk, *J. Anal. At. Spectrom.*, 2000, **15**, 383.
- 25 D. J. Douglas and J. B. French, *J. Am. Soc. Mass Spectrom.*, 1992, **3**, 398.
- 26 D. J. Douglas, *J. Am. Soc. Mass Spectrom.*, 1998, **9**, 101.
- 27 D. J. Douglas and J. B. French, Mass Spectrometer and Method and Improved Ion Transmission, US patent # 4963736, October 16, 1990.
- 28 D. W. Koppenaal, C. J. Barinaga and M. R. Smith, *J. Anal. At. Spectrom.*, 1994, **9**, 1053.
- 29 G. C. Eiden, C. J. Barinaga and D. W. Koppenaal, *J. Anal. At. Spectrom.*, 1996, **11**, 317.
- 30 G. C. Eiden, C. J. Barinaga and D. W. Koppenaal, *Rapid Commun. Mass Spectrom.*, 1997, **11**, 37.
- 31 I. Feldman, N. Jakubowski and D. Stuewer, *Fresenius' J. Anal. Chem.*, 1999, **365**, 415.
- 32 I. Feldman, N. Jakubowski, C. Thomas and D. Stuewer, *Fresenius' J. Anal. Chem.*, 1999, **365**, 422.
- 33 D. R. Bandura, V. I. Baranov and S. D. Tanner, *J. Anal. At. Spectrom.*, 2000, **15**, 921.
- 34 S. D. Tanner, V. I. Baranov and U. Vollkopf, *J. Anal. At. Spectrom.*, 2000, **15**, 1261.
- 35 D. R. Bandura, V. I. Baranov and S. D. Tanner, *Fresenius' J. Anal. Chem.*, 2001, **370**, 454.
- 36 J. S. Becker and H.-J. Dietze, *Isotopenpraxis*, 1983, **19**, 105.
- 37 P. J. Turner, D. J. Mills, E. Schroder, G. Lapitajs, G. Jung, L. A. Iacone, D. A. Haydar and A. Montaser, in *Inductively Coupled Plasma Mass Spectrometry*, ed. A. Montaser, Wiley-VCH, New York, 1998, pp. 476–479.
- 38 P. Turner, T. Merren, J. Speakman and C. Haines, in *Plasma*



- Source Mass Spectrometry: Developments and Applications*, eds. G. Holland and S. D. Tanner, Royal Society of Chemistry, Cambridge, 1997, pp. 28–34.
- 39 S. D. Tanner, V. I. Baranov and D. R. Bandura, *Spectrochim. Acta, Part B*, 2002, **57**, 1361–1452.
  - 40 J. A. McLean, H. Zhang and A. Montaser, *Anal. Chem.*, 1998, **70**, 1012.
  - 41 J. A. McLean, M. G. Minnich, L. A. Iacone, H. Liu and A. Montaser, *J. Anal. At. Spectrom.*, 1998, **13**, 829.
  - 42 J. Singh, J. A. McLean, D. E. Pritchard, A. Montaser and S. R. Patierno, *Toxicol. Sci.*, 1998, **46**, 220.
  - 43 J. Singh, D. E. Pritchard, D. L. Carlisle, J. A. McLean, A. Montaser, J. M. Orenstein and S. R. Patierno, *Appl. Pharmacol.*, 1999, **161**, 240.
  - 44 J. S. Becker, H.-J. Dietze, J. A. McLean and A. Montaser, *Anal. Chem.*, 1999, **71**, 3077.
  - 45 B. A. Acon, J. A. McLean and A. Montaser, *Anal. Chem.*, 2000, **72**, 1885.
  - 46 J. A. McLean, B. W. Acon, A. Montaser, J. Singh, D. E. Pritchard and S. R. Patierno, *Appl. Spectrosc.*, 2000, **54**, 659.
  - 47 J. A. McLean, M. G. Minnich, A. Montaser, J. Su and W. Lai, *Anal. Chem.*, 2000, **72**, 4796.
  - 48 B. W. Acon, J. A. McLean and A. Montaser, *J. Anal. Atom. Spectrom.*, 2001, **16**, 852.
  - 49 J. R. Chirinos, K. Kahen, S. E. O'Brien and A. Montaser, *Anal. Bioanal. Chem.*, 2001, **372**, 128.
  - 50 J. Speakman, P. J. Turner, A. N. Eaton, F. Abou-Shakra, Z. Palacz and R. C. Haines, The Use of Photomultiplier Detector in Routine ICP-MS, presented at European Winter Conference on Plasma Spectrochemistry, Pau, France, January 10–15, 1999.
  - 51 A. Montaser, J. A. McLean and J. M. Kacsir, A Novel Direct Injection High Efficiency Nebulizer for Atomic Spectroscopy, 1997 U.S. Patent No. 6,166,379, December 26, 2000.
  - 52 M. Horn, *Fresenius' J. Anal. Chem.*, 1999, **364**, 385.
  - 53 S. F. Boulyga and J. S. Becker, *Ber. Forschungszent. Juelich*, 2000, **Juel-3821**, 13.
  - 54 S. F. Boulyga and J. S. Becker, *J. Anal. At. Spectrom.*, 2002, **17**, 1202.
  - 55 S. D. Tanner and V. I. Baranov, *J. Am. Soc. Mass Spectrom.*, 1999, **10**, 1083.
  - 56 K. M. Ervin and P. B. Armentrout, *J. Chem. Phys.*, 1985, **83**, 166.
  - 57 S. F. Boulyga, H.-J. Dietze and J. S. Becker, *Mikrochim. Acta.*, 2001, **137**, 93.
  - 58 M. A. Dexter, P. K. Appelblad, C. P. Ingle, J. H. Batey, H. J. Reid and B. L. Sharp, *J. Anal. At. Spectrom.*, 2002, **17**, 183.
  - 59 V. Bianchi, L. Celotti, G. Lanfranchi, F. Majone, G. Marin, A. Montaldi, G. Sponza, G. Tamino and P. Venier, *Mutat. Res.*, 1983, **117**, 279.
  - 60 L. C. Bridgewater, F. C. R. Manning and S. R. Patierno, *Carcinogenesis*, 1994, **15**, 2421.
  - 61 B. W. Acon, J. A. McLean, S. E. O'Brien, S. F. Boulyga, J. S. Becker, H.-J. Dietze and A. Montaser, 'Evaluation of a Direct Injection High Efficiency Nebulizer for Use with Hexapole Collision Cell Inductively Coupled Plasma Mass Spectrometry', 5th Annual Symposium for Mass Spectrometry, September 18–22, 2000, Research Centre Juelich, Juelich, Germany.